Check for
updates

Rogue waves of the dissipative Gross–Pitaevskii equation with distributed coefficients

Emmanuel Kengne[a] [ORCID]

School of Physics and Electronic Information Engineering, Zhejiang Normal University, Jinhua 321004, China

Abstract By introducing a suitable ansatz and employing the similarity transformation technique, we construct the first- and second-order rational solutions for a quasi-one-dimensional (1D) dissipative Gross–Pitaevskii (GP) equation with a time-varying cubic nonlinearity and an external time-dependent potential. Then, by using these solutions, we engineer first- and second-order rogue waves in the Bose–Einstein condensate (BEC) contexts for the experimentally relevant systems when the gain/loss of atoms is taken into consideration. Our analysis shows that the control of the scattering length, the external harmonic, and the linear trapping potentials allows one to manage the motion and the background of dissipative rogue matter waves in BEC systems. We show that the wave amplitudes depend on the absolute value of s-wave scattering and the bias magnetic field, while its motion depends on the external trapping potentials. We show that unlike classical rogue waves, the nonzero continuous wave backgrounds of non-autonomous forced (damped) rogue matter waves in BECs with time-dependent complicated potential increases (decreases) during the wave motion. Our results also reveal that neither the gain nor the loss of the BEC atoms affects the amplitude of the rogue matter waves during their propagation. Our results may help to control and manage experimentally dissipative rogue waves in a BEC systems.

1 Introduction

Named by oceanographers to isolated large amplitude waves, rogue waves (RWs) are giant single waves that were firstly found in the oceans with amplitudes much higher than the average wave crests around them [1]; they occur more frequently than expected for normal, Gaussian distributed, statistical events. Rogue waves are ubiquitous in nature and appear in a variety of different contexts such as liquid helium, nonlinear optics, microwave cavities, nonlinear transmission lines, Bose–Einstein condensates (BECs), etc.[1–8]. Rogue waves are rare events with the key feature that they appear from nowhere and disappears without a trace [2,9,10]. RWs may arise from the instability of a certain class of initial conditions that tend to grow exponentially and thus have the possibility of increasing up to very high amplitudes reaching three times the amplitude of the unperturbed waves, due to modulational instability (MI) [11–13]. Rogue waves are, mathematically rational solutions for some nonlinear partial differential equations (NPDEs) such as the focusing nonlinear Schrödinger (NLS) equation

---

[a] e-mail: ekengne6@zjnu.edu.cn (corresponding author)

[14,15] and physically are located in both space and time, concentrating thus the energy of the background into a small region due to the nonlinear properties of the medium [11]. As rational solutions of some NPDEs, RWs vary more slowly than the usual solitons with hyperbolic functions; therefore, rogue waves may be more easily stable than standard solitons.

Because of their presence in a variety of different fields of the nonlinear science, RWs appearing as rational solutions of nonlinear partial differential equation of Schrödinger type have attracted in recent years more and more attention [15–20]. In the context of NLS equation, a number of methods including the Darboux transformation, the similarity transformation, the numerical simulation, as well as the direct approach were used to investigate the occurrence of the rogue waves and their properties [11,14,15,21–23]. It has been reported that RWs described by the first-order rational solution of the self-focusing NLS equation are robust relative to a certain class of perturbations of the NLS equation, while RWs described by the higher-order rational solutions of the self-focusing NLS equation are able to concentrate great amounts of energy into a relatively small area in space [6,11]; this property of the RWs as the higher-order rational solutions of the self-focusing NLS equation may serve as the basis for the scientific explanation of rogue waves that can, in a single action, destroy the biggest ships traveling the vast expanses of the world's oceans [1].

Since the first experimental and theoretical realizations of Bose–Einstein condensates [24–27], extensive research works carried out on the behaviors of the macroscopical quantum and dynamic evolution, matter-wave solitons, rogue waves, coherent structures, as well as domain formation of BECs trapped in optical lattices become more active and competitive than before in both experiment and theory aspects, stimulating intensive studies of the nonlinear excitations of the atomic matter waves [28–31]. As well as we know, just a few works have been reported on the analytical investigation of rogue matter wave in the context of BECs. Using numerical simulations, Bludov et al. [8] have predicted the existence of rogue matter waves in Bose–Einstein condensates either loaded into a parabolic trap or embedded in an optical lattice. The goal of the present work is to develop mathematical models that may open possibilities for generating non-autonomous rogue matter waves of BECs trapping an external time-dependent complex potentials and for detailed studies of their properties in laboratory conditions. These mathematical studies on non-autonomous rogue matter waves in BECs with feeding/loss of atoms may also help us to understand deeply the nature and the dynamics of instabilities in BECs with time-dependent potentials, especially when either the loss or the gain of atoms in the BEC system is taken into account. The rest of this paper is organized as follows. In Sect. 2, we present analytical first- and second-order rational solutions of the dissipative Gross–Pitaevskii (GP) equation with a spatiotemporal potential that may describe the Bose–Einstein condensate systems with a time-dependent complex potential, composed of a parabolic background potential, a linear magnetic and the time-dependent laser fields when either the feeding or the loss of atoms is taken into account. In Sect. 3, we use the found rational solutions to investigate qualitatively and quantitatively the properties of the non-autonomous rogue matter waves of BEC system under consideration. The main results are summarized in Sect. 4.

2 Model and analytical exact first- and second-order rational solutions of the GP equation

2.1 Description of the model

At absolute zero temperature, the properties of weakly interacting bosonic gases trapped in a potential are usually described by a distributed NLS equation with a trap potential which, in the context of BECs, is named Gross–Pitaevskii equation [32]. The cubic nonlinear term in the NLS equation, corresponding to the two-body interatomic interactions has been reported to be generally the dominant one [33] so that the three-body interatomic interactions that corresponds to the quintic term in the NLS equation and can be treated as a perturbation over the two-body case can be neglected, especially at low densities [34]. In the physically important case of the cigar-shaped trapping potential in presence of either the loss or the gain of atoms, the NLS equation can be integrated out, resulting into a dissipative quasi-one-dimensional cubic NLS equation (known as Gross–Pitaevskii equation in the BEC theory)

$$i\frac{\partial \psi}{\partial t} + \frac{1}{2}\frac{\partial^2 \psi}{\partial x^2} + g(t)\,|\psi|^2\,\psi + \left[k(t)x^2 + \lambda(t)x + i\gamma(t)\right]\psi = 0, \tag{1}$$

where $g(t), k(t), \lambda(t)$, and $\gamma(t)$ are all real functions of time t. The temporal and spatial coordinates t and x are measured respectively by harmonic-oscillator units $1/\omega_\perp$ and $a_\perp$, where $\omega_\perp$ is the harmonic-oscillator frequency and $a_\perp = \sqrt{\hbar/(m\omega_\perp)}$ and $a_0 = \sqrt{\hbar/(m\omega_0(t))}$ are the corresponding linear oscillator lengths in the transverse and cigar-axis directions, respectively, m being the atomic mass and ω_0 being the axial-oscillation frequency (in the cigar-axis direction). In our study, the radial oscillation frequency $\omega_\perp$ is considered as constant, while the axial oscillation frequency ω_0 will be considered to be time-dependent. $\psi(x, t)$ is the macroscopic wave function and is measured in units of $1/\sqrt{2\pi a_B a_\perp}$, where $a_B = a_\perp \int_{-\infty}^{+\infty} |\psi|^2\,dx / \left(2 \int_{-\infty}^{+\infty} |\Psi|^2\,d\mathbf{r}\right)$ is the Bohr radius; here, $\Psi(\mathbf{r}, t)$ is the original order parameter connected to the macroscopic wave function $\psi(x, t)$ as follows [35]

$$\Psi(\mathbf{r}, t) = \frac{1}{\sqrt{2\pi a_B a_\perp}} \psi\left(\frac{x}{a_\perp}, t\right) \exp\left[-i\omega_\perp t - \frac{y^2 + z^2}{2a_\perp^2}\right]. \tag{2}$$

Parameter $g(t) = -2a_s/(3a_B)$ of the cubic nonlinearities represents the two-body interatomic interactions coefficients, negative for repulsive interatomic interactions (defocusing nonlinearities) and positive for attractive ones (or focusing nonlinearities), while parameter a_s is the s-scattering length [36]. In the relevant experiments, a bright soliton has been created by utilizing a Feshbach resonance to manipulate the sign of the s-wave scattering length from positive to negative; in his situation, the s-wave scattering length a_s is allowed to be a function of time t. In the present study, we consider the general case of time-dependent s-wave scattering length. The quadratic term of the complex potential

$$V(x, t) = k(t)x^2 + \lambda(t)x + i\gamma(t) \tag{3}$$

is the most physically relevant example of an external potential in the BEC case, giving the harmonic confinement of atoms by experimentally used magnetic traps. The potential parameter $k(t) = \pm\omega_0^2/\left(2\omega_\perp^2\right)$ measures the strength of the magnetic trap and may be negative (confining potential) or positive (repulsive potential); it is typically fixed in current experiments, but adiabatic changes in the strength of the trap are experimentally feasible. Hence, we examine the more general time-dependent case. The linear term $\lambda(t)x$ of the complex potential (3) may correspond to the gravitational field or some linear potentials. The

time-dependent parameter $\gamma(t)$ relates the feeding ($\gamma < 0$) or loss ($\gamma > 0$) of atoms in the condensate resulting from the contact with the thermal cloud and three-body recombination [37,38]. Because the nonlinearity parameter g and the potential parameters k, λ, and γ are time-dependent functions, Eq. (1) can be used to describe the control and management of BEC system by properly choosing the four time-dependent parameters.

It is important to note that from the viewpoint of stability, the one-dimensional approximation (1) that describes the macroscopic wave function $\psi(x, t)$ is different from the three-dimensional equation that governs the original order parameter (2). For a true 1D system, one does not expect the collapse of the system when increasing the BEC number of atoms [39,40]. It happens that a realistic 1D approximation is not a true 1D system, with the density of particles still increasing due to the strong restoring forces in the perpendicular directions. Therefore, it is important to associate with the GP Eq. (1) additional conditions (limits) under which the system becomes effectively 1D, that is, the kinetic energy in the transverse direction is much greater than the energy of the two body interactions; this means that $\epsilon^2 = a_\perp/\zeta^2 \sim N|a_s|/a_0 << 1$, ζ and N being respectively the healing length and the total number of atoms [41]. Normalizing the density $|\psi(x, t)|^2$ and the energy in Eq. (1) in units of $2a_s$ and $\hbar\omega_\perp$, Eq. (1) under the condition $\epsilon^2 = a_\perp/\zeta^2 \sim N|a_s|/a_0 << 1$ becomes effectively 1D. For a concrete BEC system, we can follow the idea used in Ref. [44] to obtain a safe range of parameters. For example, the BEC bright soliton has been created for [7] Li with the parameters of $N \approx \times 10^3$, $\omega_\perp = 2\pi \times 700$ Hz, and $\omega_0 = 2\pi \times 7$ Hz, and $a_{final} = -4a_B$, which provides a safe range of parameters [44]. If we take for example $a_s(t = 0) = -0.25a_B$, we can calculate, under these experimental parameters, $\epsilon^2 = a_\perp/\zeta^2 \sim N|a_s|/a_0 = 9.5 \times 10^{-3} << 1$. Creating the BEC bright soliton in [7] Li, it has been found that $k(t) = -2\kappa^2$ with $\kappa \simeq 0.05$.

2.2 First- and second-order rational solutions of the GP Eq. (1)

In order to extract exact rational solutions of the GP Eq. (1), we look for solutions of the form

$$\psi(x, t) = [A + B\psi_1(X, T) + iC\psi_2(X, T)] \exp[i\chi + i\lambda_0 T], \quad (4a)$$

where A, B, C, and T are all function of time t, $X = X(x, t)$ and $\chi = \chi(x, t)$ are two real functions, λ_0 is a real control parameter, and ψ_1 and ψ_2 are real functions of variables X and T. Inserting Eq. (4a) into Eq. (1) and asking that ψ_1 and ψ_2 satisfy equations that do not contain explicitly X and T lead to

$$X(x, t) = \alpha(t)x + \beta(t), \quad (4b)$$

$$\chi(x, t) = -\frac{1}{2\alpha}\frac{d\alpha}{dt}x^2 - \frac{1}{\alpha}\frac{d\beta}{dt}x + \chi_0(t), \quad (4c)$$

$$(A(t), B(t), C(t)) = (A_0, B_0, C_0)\sqrt{|\alpha|}\exp\left[-\int\gamma(t)dt\right], \quad (4d)$$

where A_0, B_0, and C_0 are real constants and $(T, \alpha, \beta, \chi_0)$ is any real solution of the differential system

$$\frac{dT}{dt} - T_0\alpha^2(t) = 0, \quad T_0 \neq 0, \quad (5a)$$

$$\frac{d^2\alpha}{dt^2} - \frac{2}{\alpha}\left(\frac{d\alpha}{dt}\right)^2 + 2\alpha k = 0, \quad (5b)$$

$$\frac{d^2\beta}{dt^2} - \frac{2}{\alpha}\frac{d\alpha}{dt}\frac{d\beta}{dt} + \alpha\lambda = 0, \tag{5c}$$

$$\frac{d\chi_0}{dt} + \frac{1}{2}\left(\frac{1}{\alpha}\frac{d\beta}{dt}\right)^2 = 0. \tag{5d}$$

The choice of Eq. (5a) is made to preserve the scaling; here, T_0 is an arbitrary real parameter to be determined later. In Eq. (4b), $\alpha(t)$ is the inverse of the wave width, while $-\beta(t)/\alpha(t)$ is the position of its centre of mass. Inserting ansatz (4a) into Eq. (1) and setting the real and imaginary parts of the resulting equation equal to zero, we obtain the following sets of integrable partial differential equations for ψ_1 and ψ_2 in terms of rescaled variables X and T

$$C_0 T_0 \frac{\partial\psi_2}{\partial T} - \frac{B_0}{2}\frac{\partial^2\psi_1}{\partial X^2} + \lambda_0 T_0 (A_0 + B_0\psi_1)$$
$$- g_0 (A_0 + B_0\psi_1)\left[(A_0 + B_0\psi_1)^2 + C_0^2\psi_2^2\right] = 0, \tag{6a}$$

$$B_0 T_0 \frac{\partial\psi_1}{\partial T} + \frac{C_0}{2}\frac{\partial^2\psi_2}{\partial X^2} - C_0\lambda_0 T_0\psi_2$$
$$+ C_0 g_0 \psi_2 \left[(A_0 + B_0\psi_1)^2 + C_0^2\psi_2^2\right] = 0, \tag{6b}$$

if $\alpha(t)$ is taken from the condition

$$g_0^2\alpha^2 - g^2 \exp\left[-4\int\gamma(t)dt\right] = 0, \quad g_0 \neq 0 : g_0 g(t) > 0, \tag{7}$$

and if the nonlinearity parameter $g(t)$ and the potential parameters $k(t)$ and $\gamma(t)$ satisfy the condition

$$g\frac{d^2g}{dt^2} - 2\left(\frac{dg}{dt}\right)^2 + 2g^2 k - 2g\left(g\frac{d\gamma}{dt} - 2\gamma\frac{dg}{dt} + 2g\gamma^2\right) = 0. \tag{8}$$

In Eq. (7), g_0 is an arbitrary real parameter having the same sign as $g(t)$ to be determined later. That is to say, the GP Eq. (1) in terms of rescaled variables X and T is converted to system (6a)–(6b) when the nonlinearity parameter $g(t)$, the harmonic trapping potential parameter $k(t)$, and the linear trapping potential parameter $\gamma(t)$ satisfy the condition (8) which will be, in what follows, referred to as the integrable condition.

Thus, the virtue of the suitable ansatz (4a) is that with relatively less complicated calculation, we not only establish the integrable condition (8) for the GP Eq. (1), but also retrieve the system of nonlinear partial differential Eqs. (6a)–(6b), which may be used to investigate various properties of the BEC system under consideration. It is important to note that Eq. (5b) is satisfied as soon as α is given by Eq. (7) and $g(t)$, $k(t)$, and $\gamma(t)$ satisfy the integrable condition (8).

Following Akhmediev et al. [15], system (6a)–(6b), we find for the first-order rational solution,

$$\psi_1(X, T) = -\frac{4}{B_0 \left(1 + 2X^2 + 4T^2\right)}, \quad \psi_2(X, T) = -\frac{8T}{C_0 \left(1 + 2X^2 + 4T^2\right)}. \tag{9}$$

Inserting Eq. (9) into Eq. (4a) and using Eqs. (4b)–(4d) yield the following first-order rational solution of the GP Eq. (1)

$$\psi(x, t) = \sqrt{2g(t)} \exp\left[-2\int\gamma(t)dt\right]\left[1 - \frac{4 + i8T}{1 + 2\left[\alpha(t)x + \beta(t)\right]^2 + 4T^2}\right]\exp\left[i\chi + iT\right]. \tag{10}$$

Because $g_0 = \frac{1}{2}$ and $g_0 g(t) > 0$ (see condition (7) and the Appendix), the first-order rational solution of the GP Eq. (1) is associated to BECs with attractive interatomic interactions.

Taking for simplicity $A_0 = \lambda_0 = 1$, $g_0 = \frac{1}{2}$, and $T_0 = \frac{1}{2}$ and employing again the direct method developed in Ref. [15], we find the below second-order rational solution of system (6a)–(6b)

$$\psi_1(X, T) = \frac{\psi_{11}(X, T)}{\psi_{12}(X, T)}, \quad \psi_2(X, T) = \frac{\psi_{22}(X, T)}{\psi_{21}(X, T)}, \tag{11a}$$

where ψ_{11}, ψ_{ij}, and $\psi_{22}(X, T)$ are given in Eq. (A1) of the appendix. Inserting Eqs. (11a) and (A1) into Eq. (4a) and using Eq. (4d) lead to the following second-order rational solution of the GP Eq. (1)

$$\psi(x, t)$$
$$= \left[1 + \frac{3\left(1 - 4X^2\right) + 8T^2\left(8T^2 - 9\right) - 4\left(X^2 + 6T^2\right)^2 + 2i\left\{15 - 8T^2 + 12X^2 - \left(4T^2 + 2X^2\right)^2\right\}}{8\psi_{12}(X, T)} \right]$$
$$\times \sqrt{2g} \exp\left[-2 \int \gamma(t)dt\right] \exp\left[i\chi(x, t) + iT(t)\right]. \tag{12}$$

3 Control and management of dissipative rogue matter waves in BECs with complicated potential

In this section we show how the GP Eq. (1) can be used to describe the control and management of BECs with complicated potential by properly choosing the nonlinearity parameter $g(t)$ and the three time-dependent parameters $k(t)$, $\lambda(t)$ and $\gamma(t)$ of the complex potential (3). Because the control of rogue waves in BEC systems under a harmonic potential with gain/loss or a real second-order polynomial potential have already been discussed in the literature with analytical results (see for example Refs. [42] and [43]), we focus ourselves more on BEC systems for which both the linear term and gain/loss are taken into consideration. Because the methodology used to derive the above rogue wave solutions of the GP Eq. (1) with potential (3) is based neither on the standard NLS equation nor on the Hirota Bilinear Method [42], it is important to investigate, when using these exact solutions, the control and management of dissipative ($\gamma(t) \neq 0$) rogue matter waves in BEC systems in both the situation when linear term of potential (3) is absent ($\lambda(t) = 0$) and the situation when potential (3) contains the linear term ($\lambda(t) \neq 0$). Because we are interested in dissipative rogue matter waves, we will not investigate the case of BECs in second-order polynomial potential [43].

As we can see from the first- and the second-order rational solutions (10) and (12), the amplitude of the rogue matter waves found in this work is proportional to $p(t) = \sqrt{2g(t)} \exp\left[-2 \int \gamma(t)dt\right]$ which depends on both the feeding (loss) parameter $\gamma(t)$ and the s-wave scattering length. Therefore, the wave amplitude increases (decreases) with time if function $p(t)$ increases (decreases) with time t [because the maximum value of the main peak of the rogue wave is unique, that is, is reached at one and only one time $\tilde{t}$, this maximum remains constant during the wave propagation, so that during the rogue wave evolution, one can only observe how its background density either increases or decreases, depending on the behavior of $p(t)$].

As we have already mentioned, it follows from Eq. (4b) that the width on the rogue matter wave under investigation is inversely proportional to $\alpha(t)$, while its centre of mass, obtained
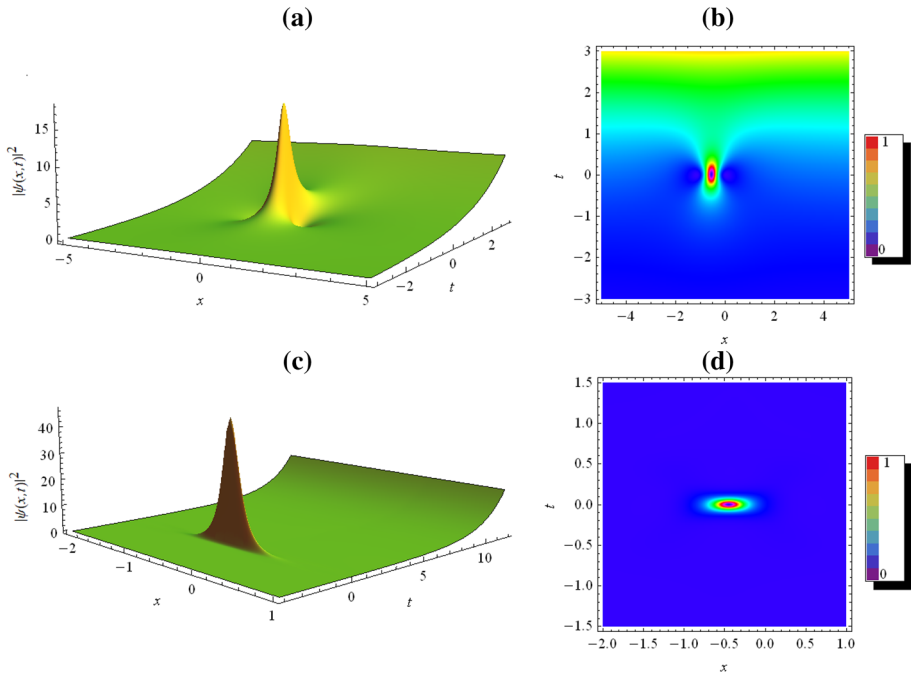
Fig. 1 Evolution of the atomic density **a**, **c** and density plot for the density $|\psi(x,t)|^2$ associated respectively to **a**, **b** the first-order rational solution (10) and **c**, **d** the second-order rational solution (12) of the GP Eq. (1). To generate different plots, we have used the gain parameter $\gamma(t) = \gamma_-$ with solution data (A2) for $\beta_{01} = 1.0$ and $\beta_{02} = 0.1$.

by setting $X(x,t) = 0$, is $\xi(t) = -\beta(t)/\alpha(t)$ and satisfies the following equation

$$\frac{d^2\xi}{dt^2} - 2k\xi - \lambda = 0. \tag{13}$$

Indeed,

$$\frac{d\xi(t)}{dt} = -\frac{1}{\alpha^2}\left(\alpha\frac{d\beta}{dt} - \beta\frac{d\alpha}{dt}\right), \quad \frac{d^2\xi}{dt^2} = \frac{1}{\alpha}\left[\frac{2}{\alpha}\frac{d\alpha}{dt}\frac{d\beta}{dt} - \frac{2}{\alpha^2}\beta\left(\frac{d\alpha}{dt}\right)^2 + \frac{\beta}{\alpha}\frac{d^2\alpha}{dt^2} - \frac{d^2\beta}{dt^2}\right].$$

Replacing $\frac{d^2\alpha}{dt^2}$ and $\frac{d^2\beta}{dt^2}$ by their expression from Eqs. (5b) and (5c) and using the definition of $\xi(t)$ lead to Eq. (13). Equation (13) of the centre of mass of the macroscopic wave packet shows that we can manipulate the motion of rogue matter waves in the BEC system under consideration by controlling both the external harmonic and linear trapping potentials. In what follows, we take some examples to demonstrate the engineering of rogue matter waves in one-dimensional BEC systems with different kinds of scattering length and complex trapping potential. In our simulations, we will, without loss of generality, consider only positive $\alpha(t)$ from Eq. (7).

3.1 Engineering of dissipative rogue matter waves in BEC system with time-independent harmonic confining potential

As the first example, we consider the time-independent harmonic potential similar to the one used by Khaykovich et al. [44] in the creation of bright BEC solitons. In that experiment, authors used $\omega_\perp = 2\pi \times 700\,\text{Hz}$ and $\omega_0 = 2\pi \times 7\,\text{Hz}$, leading to $k(t) = -2\kappa^2$ with $\kappa \simeq 0.05$. For such a time-independent harmonic potential, Wu et al. [45] employs the parameter $g(t) = \exp[\pm 2\kappa t]$ of the s-wave scattering length to investigate the dynamics of bright solitons in BECs with time-independent harmonic potential when gain/loss of atoms as well as the linear potential were ignored. In the present example, we neglect the linear potential, setting $\lambda(t) = 0$, and take into account the gain (loss) of atoms in the condensate. Inserting the above $g(t)$ and $k(t)$ into the integrable condition (8) leads to the following special gain and loss parameters

$$\gamma(t) = \gamma_- = \kappa - \frac{1}{2}\sqrt{2k} \text{ and } \gamma(t) = \gamma_+ = \kappa + \frac{1}{2}\sqrt{2k}. \tag{14}$$

The corresponding $\alpha(t)$, $\beta(t)$, and $T(t)$ are given in the appendix (see Eqs. (A2) and (A3)). While in any experiment the time is considered positive, to avoid introducing a time shift in Eqs. (A2) and (A3), which would be less convenient for the analytical arguments, we assume that the experiment starts at non-positive initial time, that is, at $t_0 \leq 0$. We also assume the $|t_0| >> 1$ so that the initial homogeneous density distribution is only weakly modulated [8].

With the above consideration on the initial time, the amplitude of the each of the first-order and the second-order rogue matter waves given respectively by Eqs. (10) and (12) has its maximum at $t \simeq 0$. This is well seen from Fig. 1 showing the evolution of the atomic density [1(a), 1(c)] and the density plots [1(b), 1(d)] according respectively to the first-order rational solution (10) and the second-order rational solution (12). From plots of this Fig. 1, it can be seen that with the increasing of the absolute value of the s-wave scattering length associated to BECs with feeding of atoms, the rogue matter wave has an increase in the peaking value. We can also see from Fig. 1 that the first- and second-order rogue matter waves associated to BECs with feeding of atoms are localized in both the t and x directions, meaning that they appear from nowhere and disappear without trace. This behavior also means that the rogue matter waves can concentrate the energy of the BEC system with gain of atoms in a small region. Unlike rogue matter waves of the NLS equation, it is seen from plots of Fig. 1 that the nonzero continuous wave (cw) backgrounds of the waves increase (this is well observed in Fig. 1(a)) because of the presence of the forcing dissipative term γ in Eq. (1). However, the backgrounds of the waves decrease when $\gamma(t) = \gamma_+ > 0$ (loss of atoms) (for simplicity, we do not include the figures corresponding to the BEC with loss of atoms here). Therefore, with the increasing (decreasing) of the absolute value of the s-wave scattering length, the rogue matter wave has an increase (decrease) in the nonzero background.

3.2 Generation of dissipative rogue matter waves in BEC system with the temporal periodic modulation of the s-wave scattering length

Some years ago, it has been shown that one can introduce certain free (suitable) parameters in the rogue wave solutions which allow one to split the symmetric form solution into a multi-peaked solution and that by varying these free parameters one can extract certain novel patterns of rogue waves [46]. Motivated by this, in the following, we follow Saito and Ueda [47] and consider the temporal periodic modulation of the s-wave scattering length with the strength of interaction oscillating rapidly at frequency ω; such a variation of the atomic
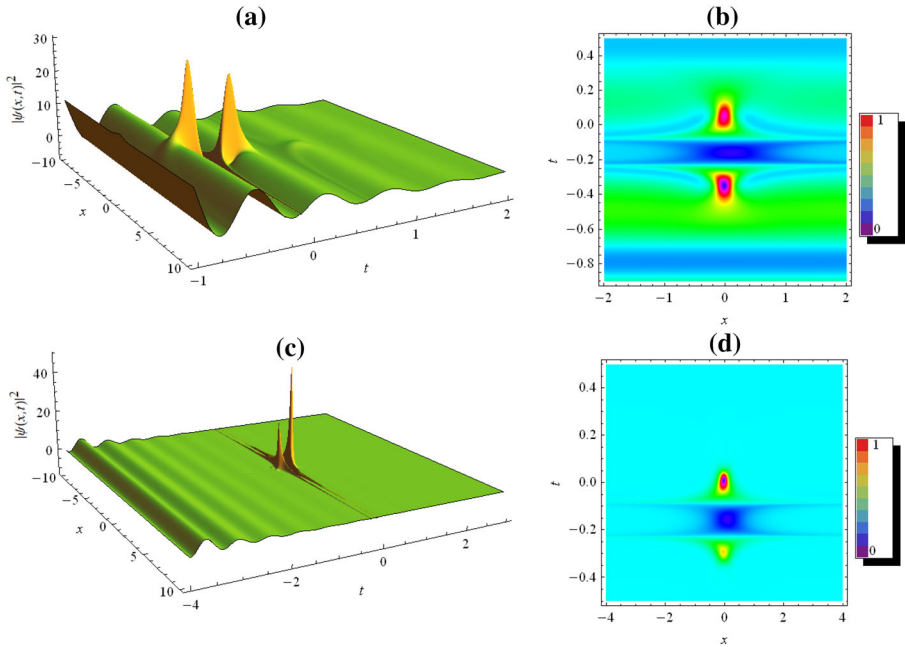
(a)

(b)

(c)

(d)

Fig. 2 Evolution of the atomic density **a**, **c** and density plots of the density $|\psi(x, t)|^2$ **b**, **d** according to **a**, **b** the exact analytical first-order rational solution (10) and **c**, **d** exact analytical second-order rational solution (12) of the GP equation (1) for $\beta_{01} = \beta_{02} = -0.01$, $\gamma = 0.3$, $m = 1.3$, and $\omega = 10$

scattering length can be achieved experimentally either by varying the magnetic field or by using optically induced Feshbach resonances [48,49]. We thus consider the GP equation with the nonlinearity parameter $g(t) = 1 + m \sin[\omega t]$, $0 < m < 1$. In this example, we ignore the linear potential (that is, $\lambda(t) = 0$) and, following Kengne and Talla [38], consider the gain (loss) parameter to be time-independent, that is, $\gamma(t) = \gamma$ is a real constant. Imposing to g and γ to satisfy the integrable condition (8) leads to the temporal periodic modulation of the trapping potential with strength

$$k(t) = 2\gamma \left(\gamma - \frac{1}{g}\frac{dg}{dt}\right) + \frac{1}{g^2}\left(\frac{dg}{dt}\right)^2 - \frac{1}{2g}\frac{d^2g}{dt^2}. \tag{15}$$

Integrating system (5b)–(7) leads to the $\alpha(t)$, $\beta(t)$, and $T(t)$ showed in Appendix (A4). For this example, the suitable free parameters are γ, m, ω and the constants of integration β_{01}.

It should be noted that in the definition $\gamma(t) = \gamma$ of the gain (loss) parameter, $\gamma \neq 0$ is of any sign, that is, can be taken either positive (loss of atoms) or negative (feeding of atoms). With the solution parameters given in Appendix (A4) and for positive γ (case of BEC with loss of atoms), we show in Fig. 2 the evolution of the atomic density (left panels) and the density plots for the density $|\psi(x, t)|^2$ (right panels) according to the first-order (top panels) and the second-order (bottom panels) rational solutions (10) and (12). Due to the temporal periodic modulation of the s-wave scattering length and trapping potential, the rogue matter waves propagate on a modulated nonzero backgrounds. It is also seen from Fig. 2 that the nonzero backgrounds of the waves decrease because of the loss of atoms in the condensate. We note that the nonzero backgrounds of the waves will increase with for BEC system with gain of atoms (for simplicity we have not included the figures here. We also observe the
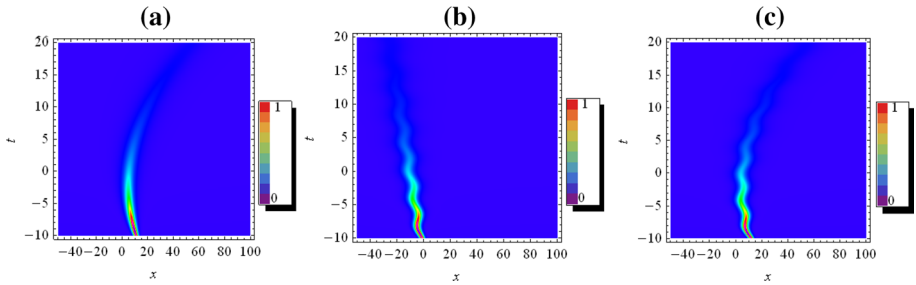
Fig. 3 Evolution of the second-order rogue matter waves according to the exact second-order rational solution (12) of the GP Eq. (1) for $g = 1$ and for the solution parameters $\beta_{01} = 0.8$, $\beta_{02} = -0.2$, and $\gamma_{01} = 25$. **a**: Evolution of the second-order rogue wave according to Eq. (12) under the effect of bias magnetic field; the parameters are $\sigma = 0.2$ and $m = 0$. **b**: Evolution of the second-order rogue wave according to Eq. (12) under the effect of laser field; the parameters are $\sigma = 0$, $m = 1$, and $\omega = 1.5$. **c**: Evolution of the second-order rogue wave according to Eq. (12) under the combined effect of bias magnetic and laser fields; the parameters are $\sigma = 0.2$, $m = 1$, and $\omega = 1.5$

emergence of the two distinct neighbor rogue waves with different amplitude for each of the first- and second-order rational solutions (10) and (12).

3.3 Transmission dissipative rogue matter wave in BEC trapped in a temporal periodic modulated linear complex potential

As the third example, we consider a BEC trapped in a temporal periodic modulated linear complex potential, meaning that $k(t) = 0$ and $\lambda(t)\gamma(t) \neq 0$ in Eq. (1). If we consider that the Bose–Einstein condensate under investigation is trapped in the coupling external magnetic field and a laser field, then the strength $\lambda(t)$ of the linear potential can be expressed as followed [50–52]

$$\lambda(t) = \sigma + m \cos[\omega t], \qquad (16)$$

where σ and m are the strengths of the linear magnetic field and the time-dependent laser field, respectively. The intensity of the laser light field is periodically modulated in time with modulation frequency ω. In what follows, we distinguish two cases, the case of BECs with a time-independent s-wave scattering length and the case of BECs with a time-dependent s-wave scattering length.

3.3.1 Case of BECs with a time-independent s-wave scattering length

Let us consider a BEC with a time-independent s-wave scattering length, which is associated with a GP Eq. (1) with a constant nonlinearity parameter g. Employing Eqs. (5b)–(8) yields

$$\gamma(t) = \frac{1}{2t + \gamma_{01}}, \quad \alpha(t) = \frac{2g}{2t + \gamma_{01}}, \quad T(t) = \frac{2g^2 t}{\gamma_{01}(2t + \gamma_{01})},$$

$$\beta(t) = \beta_{01} - \frac{\sigma g}{2}t - \frac{g(8g\beta_{02} + \sigma\gamma_{01}^2)}{4(2t + \gamma_{01})} + \frac{2gm}{\omega^2}\frac{\cos[\omega t]}{2t + \gamma_{01}}, \qquad (17)$$

where γ_{01}, β_{01}, and β_{02} are three arbitrary real constants (it is preferable to use β_{01} and β_{02} which satisfy the condition $|\beta(t)| > 0$); γ_{01} must be taken from condition $t \neq -\gamma_{01}/2$, for all $t \geq t_0, t_0 \leq 0$ being the initial time. It should be noted that $\gamma(0) = \frac{1}{\gamma_{01}}$ is the initial magnitude of the feeding/loss parameter $\gamma(t)$ so that γ_{01} will play, as we will see in what follows, an
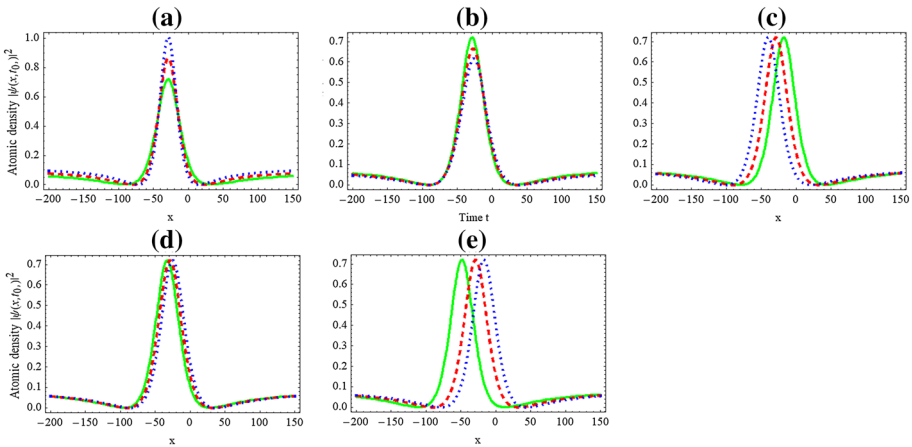
Fig. 4 Variation of the first-order rogue wave solution (10) at the time $t_0 = 0$ with the solution parameters are $\beta_{01} = \beta_{02} = 0$ for different values of **a** the nonlinearity parameter g, **b** the loss parameter γ_{01}, **c** the laser field parameter m, **d** the parameter σ of the magnetic field, and **e** the laser frequency ω. **a**: Effects of the nonlinearity parameter g on the wave propagation with $m = 4.0$, $\omega = 0.30$, $\sigma = 0.20$ and $\gamma_{01} = 25.0$ for $g = 0.25$ (solid line), $g = 0.30$ (dashed line), and $g = 0.35$ (dotted line). **b** Effects of the loss parameter γ_{01} on the wave propagation with $m = 4.0$, $\omega = 0.30$, $\sigma = 0.20$, and $g = 0.25$ for $\gamma_{01} = 25.0$ (solid line), $\gamma_{01} = 26.0$ (dashed line), and $\gamma_{01} = 27.0$ (dotted line). **c**: Effects of the laser parameter m on the wave propagation with $\omega = 0.30$, $\sigma = 0.20$, $g = 0.25$, and $\gamma_{01} = 25.0$ for $m = 3.90$ (solid line), $m = 3.95$ (dashed line), and $m = 4.0$ (dotted line). **d**: Effects of the bias magnetic parameter σ on the wave propagation with $m = 4.0$, $\omega = 0.30$, $g = 0.25$, and $\gamma_{01} = 25.0$ for $\sigma = 0.15$ (solid line), $\sigma = 0.20$ (dashed line), and $\sigma = 0.25$ (dotted line). **e**: Effects of the laser modulation frequency ω on the wave propagation with $m = 4.0$, $\sigma = 0.20$, $\gamma_{01} = 25.0$, and $g = 0.25$ for $\omega = 0.25$ (solid line), $\omega = 0.30$ (dashed line), and $\omega = 0.35$ (dotted line)

important role in the dynamics of rogue waves in BEC under consideration. For realistic Ultracold experiments, this parameter γ_{01} must be taken from condition $|\gamma(t)| \ll 1$ (that is, so that $\gamma(t)$ remains very small in absolute value). For the BEC under consideration, the amplitude of the first- and second-order rogue wave is proportional, as we can see from Eqs. (10) and (12), to $p(t) = \sqrt{2g} \exp\left[-2 \int \gamma(t) \mathrm{d}t\right] = \sqrt{2g} |2t + \gamma_{01}|^{-1}$. Therefore, the wave amplitudes increases (decreases) when parameter γ_{01} of the gain/loss of atoms decreases (increases).

With the linear potential given by Eq. (16), it is obvious that both the first- and the second-order rogue matter waves associated respectively with the first- and second-order rational solutions (10) and (12) are significantly affected by variations of the strengths σ and m of the linear magnetic field and the time-dependent laser field. This is well seen from plots of Fig. 3 showing the evolution of the second-order rogue matter wave according to Eq. (12) under the effect of (a) the bias magnetic field, (b) the laser field, and (c) both bias magnetic and laser fields. The choice of γ_{01} in this Fig. 3 makes $\gamma(t)$ positive so that the situation showed in Fig. 3 corresponds to BEC system with loss of atoms. Therefore, the wave amplitude decreases during its motion. As we can see from Fig. 3a, the wave packet, in the absence of the laser field ($m = 0$), moves in the (x, t) space along a parabolic in the $+x$ direction (the wave will travel in the $-x$ direction for $\sigma < 0$); moreover, the wave motion is uniformly accelerated, and the acceleration coincides, as we can see from Eq. (13), with the strength λ of the external potential. When either the bias magnetic field is weak ($\sigma = 0$) or both the bias magnetic and laser fields are strong ($m\sigma \neq 0$), the trajectory oscillates with frequency ω

and moves with the temporal periodic acceleration $\ddot{\xi} = \lambda = \sigma + m \cos[\omega t]$; oscillations that presents the wave motion here are induced by the laser field. In the situation when $m\sigma \neq 0$, these oscillations, as we can well seen from Fig. 3c, are around the parabolic trajectory in the $+x$ direction created by the linear magnetic field; when $\sigma = 0$ and $m \neq 0$, these oscillations are around a linear trajectory in the $-x$ direction as we can see from Fig. 3b.

As we can see from plots of Fig. 4, the first-order rogue wave solution (10) is significantly affected by the variations of the nonlinearity parameter g, the gain (loss) parameter γ_{01}, the laser field parameter m, the parameter σ of the magnetic field, as well as the laser frequency ω. Different plots of this Fig. 4 reveal that (i) the wave amplitude increases as the nonlinearity parameter g increases, as we can see from Fig. 4a. (ii) The amplitude of the first-order dissipative damped rogue wave decreases with increasing of the loss parameter γ_{01} (Fig. 4b). This means that increasing the values the loss parameter γ_{01} can reduce the nonlinearity of the BEC system, so the pulses of the dissipative rogue matter wave become shorter. (iii) The velocity of the centre of mass of the wave packet, which here is estimated by the shift of the peak position, decreases with the increasing of the parameter m of the laser field (Fig. 4c). (iv) The velocity of the centre of mass of the wave packet increases with the increasing either parameter σ of the bias magnetic field or the laser modulation frequency ω (Figs. 4d and 4e).

3.3.2 Case of BECs with a time-dependent s-wave scattering length

We now turn to the generation of rogue matter waves in BECs with a time-dependent s-wave scattering and a temporal periodic modulated linear complex potential. Following Kengne and Talla [38], we consider a condensate with a time-dependent s-wave scattering length leading to the nonlinearity parameter $g(t) = g_{01} \exp[\kappa t]$ with $g_{01} |\kappa| > 0$. Using the same gain (loss) parameter $\gamma(t) = \kappa/2$ as in Ref.[38], one easily verifies that the integrable condition (8) is satisfied. Using now Eqs. (5b)–(7) yields

$$\alpha(t) = 2g_{01}, \quad \beta(t) = \beta_{01} + 4g_{01}^2 \beta_{02} t - g_{01}\sigma t^2 + \frac{2g_{01}m}{\omega^2} \cos[\omega t], \quad T(t) = 2g_{01}^2 t, \quad (18)$$

where β_{01} and β_{02} are two arbitrary real constants to be taken from the condition that $|\beta(t)| > 0$. For such a BEC system, the amplitude of the first- and second-order rogue matter waves, as we can see from Eqs. (10) and (12), is proportional to $p(t) = \sqrt{2g(t)} \exp\left[-2 \int \gamma(t)dt\right] = \sqrt{2g_{01}} \exp\left[-\frac{\kappa}{2}t\right]$. Therefore, the wave amplitude decreases (increases) when either the s-wave scattering length $\kappa > 0$ increases (decreases) or the s-wave scattering length $\kappa < 0$ decreases (increases).

Like in the previous example, different potential's parameters as well as the parameter of the s-wave scattering length significantly affect the dissipative rogue wave motion. For a better understanding, we depict in Figs. 5 and 6 the evolution of respectively the first-order and the second-order rational solutions (10) and (12) for a negative $\gamma(t)$, showing the dynamics of dissipative forced rogue matter waves propagating in the BEC system with a time-dependent s-wave scattering and a temporal periodic modulated linear potential when the feeding of atoms is taken into consideration. From plots of Fig. 5, we can observe that: (i) The first-order dissipative forced rogue waves are localized in both the t and x directions, showing that the waves can concentrate the energy of the BEC system system in a small region. We observe from plots 5(a), 5(b), and 5(c) that each of the waves appears from nowhere, propagates and emerges into a rogue wave and then, propagates and disappears without trace. (ii) Unlike classical rogue waves, the nonzero continuous backgrounds of the waves increase because of the presence of the forcing dissipative term (in the case of BEC with loss of atoms, the nonzero continuous backgrounds of the dissipative damped rogue
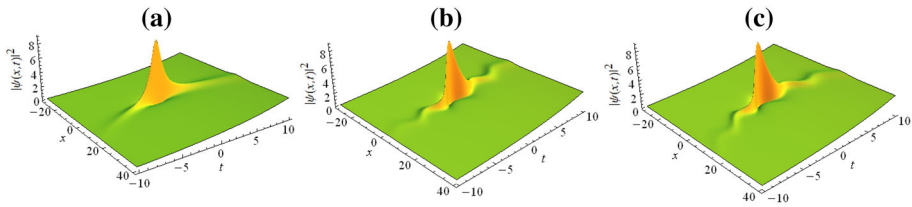
Fig. 5 Spatiotemporal evolution of the first-order dissipative forced rogue wave associated with the first-order rational solution (10) of the GP Eq. (1) with $g_{01} = 0.5$ and $\gamma(t) = -0.05$ (case of forcing term in the GP Eq. (1)) for the solution parameters $\beta_{10} = 0.1$ and $\beta_{02} = 0.2$. **a** Evolution of a first-order dissipative forced rogue wave under the effect of bias magnetic field with $\sigma = 0.25$. **b** Evolution of a first-order dissipative forced rogue wave under the effect of laser field with $m = 4$ and $\omega = \pi/2$. **c** Evolution of a first-order dissipative forced rogue wave under the combined effect of the bias magnetic and laser fields with $\sigma = 0.25$, $m = 4$ and $\omega = \pi/2$

waves will decrease during the wave propagation). (iii) Under the only bias magnetic field (that is, when the laser field is absent), the dissipative forced rogue matter wave propagates, as we can see from Fig. 5a, along a parabolic trajectory in the $+x$ direction, with acceleration $\ddot{\xi} = \sigma$ similar to the one associated with the gravity. (iv) When the bias magnetic field is neglected and only the laser field acts, the center of mass of the rogue wave oscillates due to the temporal periodic modulation of the potential and the waves propagate, as we can see from Fig. 5b, along an oscillating trajectory (these oscillations are around a linear trajectory). (v) When both the bias magnetic and laser fields act simultaneously, the dissipative forced rogue waves propagate, as we can see from Fig. 5c, along an oscillating parabolic trajectory in the $+x$ direction. The oscillations of the centre of mass of the wave packet in this situation are caused by the laser field, while the parabolic form of the trajectory is caused by the bias magnetic field.

From Fig. 6, we can well see that the second-order dissipative damped rogue wave associated with the second-order rational solution expressed by Eq. (12) is significantly affected by variations of the nonlinearity parameter g_{01} as well as the potential parameter σ, m, and ω: Plots 6(a) and 6(b) indicate that the amplitude of the dissipative damped rogue wave increases with increasing the parameter g_{01} of the s-wave scattering length and the bias magnetic parameter σ. This means that increasing the values of g_{01} and the bias magnetic parameters can enhance the nonlinearity of the BEC system and concentrate the energy in a small region, which increases the amplitude of the pulses. Therefore, the bias magnetic field enhances the nonlinearity of the BEC system. Increasing the value the laser parameter m (laser modulation frequency ω) decreases (plot 6(c)) [increases (plot 6(d))] the dissipative damped rogue wave velocity. Therefore the laser parameter m and the laser modulation frequency ω have opposite effect on the velocity of the second-order dissipative rogue wave.

3.4 Management of dissipative rogue matter waves in BEC system trapped in combined time-independent harmonic repulsive and modulated linear potentials

As our last example, we investigate the management of dissipative rogue matter waves in BEC trapped in combined time-independent harmonic repulsive and modulated linear potentials. The time-independent harmonic repulsive potential used in this example is similar to that was used in the creation of bright BEC solitons [44], with strength $k(t) = -2\kappa^2$ ($\kappa \neq 0$) of the magnetic trap. For such a strength of the magnetic trap, we follow Wu et al. [45] and consider the time-dependent s-wave scattering length leading to parameter $g(t) = g_{01} \exp[-2\kappa t]$
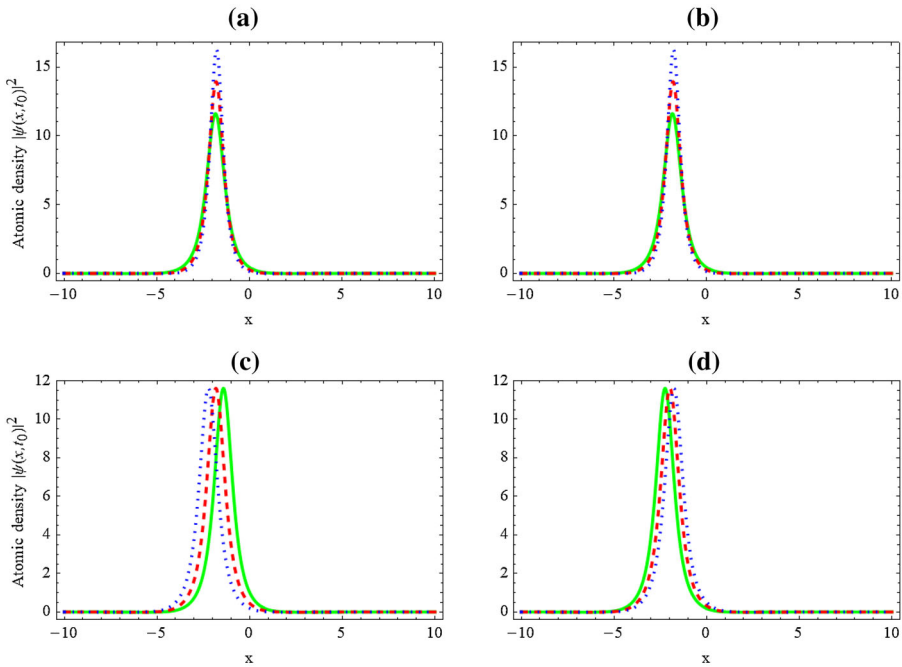
(a)

(b)

(c)

(d)

Fig. 6 Variation of the second-order rational solution (12) of the GP Eq. (1) with $\gamma(t) = 0.05$ and $\kappa = 0.1$ for solution parameters $\beta_{01} = 0.1$ and $\beta_{02} = 0.2$, showing the effect of **a** the nonlinearity parameter g_{01}, **b** the bias magnetic parameter σ, **c** the laser parameter m, and **d** the laser modulation frequency ω on the second-order dissipative damped rogue wave associated with the second-order rational solution (12) of the GP Eq. (1). **a**: Effect of the nonlinearity parameter g_{01} on the wave propagation for $\sigma = 0.25$, $m = 4$, $\omega = \pi/2$, and $g_{01} = 0.25$ (solid line), $g_{01} = 0.30$ (dashed line), and $g_{01} = 0.35$ (dotted line). **b**: Effect of the bias magnetic parameter σ on the wave propagation for $g_{01} = 0.25$, $m = 4$, $\omega = \pi/2$, and $\sigma = 0.25$ (solid line), $\sigma = 0.30$ (dashed line), and $\sigma = 0.35$ (dotted line). **c**: Effect of the laser parameter m on the wave propagation for $g_{01} = 0.25$, $\sigma = 0.25$, $\omega = \pi/2$, and $m = 3$ (solid line), $m = 4$ (dashed line), and $m = 5$ (dotted line). **d**: Effect of the laser modulation frequency ω on the wave propagation for $g_{01} = 0.25$, $\sigma = 0.25$, $m = 4$, and $\omega = 1.4$ (solid line), $\omega = 1.5$ (dashed line), and $\omega = 1.6$ (dotted line). Different plots show the wave profile at time $t_0 = 0$

(with $g_{01} > 0$) of the two-body interatomic interactions. We assume that the linear part $\lambda(t)x$ of potential (3) is some linear potentials induced by both a bias magnetic field with strength σ and a laser field with strength m and with modulation frequency ω so that $\lambda(t) = \sigma + m\cos[\omega t]$ [50–52]. Asking that $k(t)$ and $g(t)$ satisfy the integrability condition (8) yields the time-independent feeding (loss) parameter $\gamma(t) = -2\kappa$ [38]. Employing now Eqs. (5b)–(7) yields

$$\alpha(t) = 2g_{01}\exp[2\kappa t], \quad T(t) = -\frac{g_{01}^2}{2\kappa}\left(1 - \exp[4\kappa t]\right),$$

$$\beta(t) = \beta_{01} + g_{01}\left(\frac{\sigma}{2\kappa^2} + \frac{2m}{\omega^2 + 4\kappa^2}\cos[\omega t] + \beta_{02}\frac{g_{01}}{\kappa}\exp[2\kappa t]\right)\exp[2\kappa t], \quad (19)$$

where β_{01} and β_{02} are two arbitrary real constants satisfying the condition $|\beta(t)| > 0$. Because the width of the rogue wave investigated in this work is inversely proportional to $\alpha(t)$, Eq. (19) reveals that for the BECs with feeding of atoms (that for positive κ), the wave
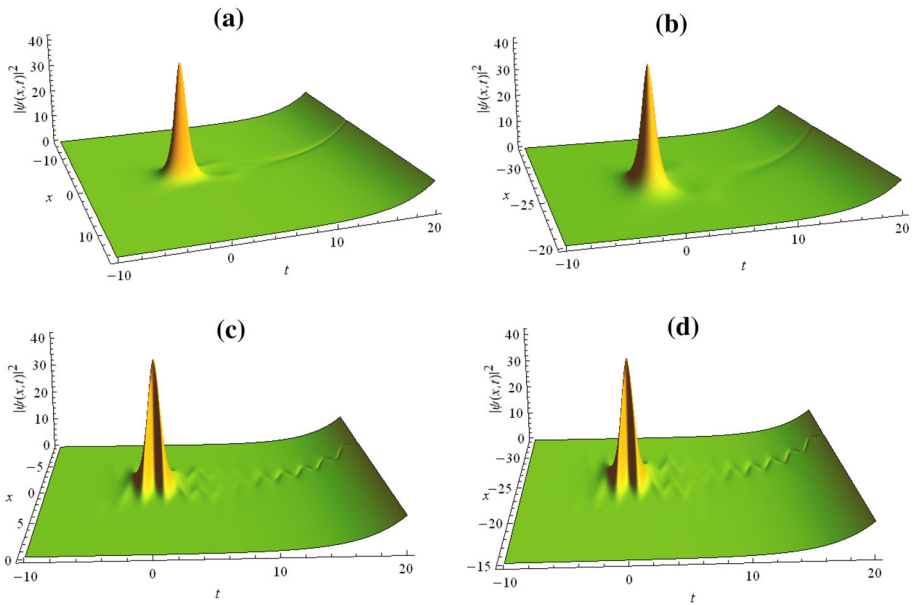
Fig. 7 Spatiotemporal evolution of the dissipative forced second-order rogue matter waves associated with the second-order rational solution (12) of the GP Eq. (1) for data (19) with $g_{01} = 0.25$ and $\kappa = 0.05$ [44] for the solution parameters $\beta_{01} = 0.1$ and $\beta_{02} = 0.2$. **a**: Evolution of the dissipative forced second-order rogue wave for BECs in the time-independent harmonic repulsive potential in the absence of both the bias magnetic and laser field ($\sigma = m = 0$). **b**: Evolution of the dissipative forced second-order rogue wave for BECs in the time-independent harmonic repulsive potential under the effect of only the bias magnetic field ($m = 0$) with $\sigma = 0.25$. **c**: Evolution of the dissipative forced second-order rogue wave for BECs in the time-independent harmonic repulsive potential under the effect of only the laser field ($\sigma = 0$) with $m = 5$ and $\omega = 3$. **d**: Evolution of the dissipative forced second-order rogue wave for BECs in the time-independent harmonic repulsive potential under the combined effects of the bias magnetic and laser fields with $\sigma = 0.25$, $m = 5$ and $\omega = 3$

width in the present example will decrease as the wave propagates and will increase with an decreasing the values of parameter g_{01} of the two-body interatomic interactions.

For the data showed in Eq. (19), we present in Fig. 7 the dynamics of the second-order dissipative forced rogue matter waves associated with the second-order rational solution (12) of the GP Eq. (1) in presence of a dissipative forcing term $\gamma(t) = -0.1$ (that is, for $\kappa = 0.05$ [44]). Figure 7a shows the spatiotemporal evolution of the wave in the case of the absence of the linear potential ($\sigma = m = 0$), Fig. 7a shows the evolution second-order rogue wave for the linear potential in the absence of the laser field, that is, when the linear potential $\lambda(t)$ consists of only the bias magnetic field with strength σ ($m = 0$). For the wave showed in Figs. 7c and 7d, the laser field is taken into consideration; Figs. 7c and 7d present the spatiotemporal evolution of the under respectively the effect of the laser field only (that is, $\sigma = 0$) and the combined effects of the bias magnetic and laser fields. For these four cases, the second-order dissipative forced rogue waves propagate on nonzero increasing backgrounds (due to the presence of the forcing dissipative term) and are localized in both the time t and the space x so that the dissipative forced rogue matter waves can concentrate the energy of the BEC system in a small region, as it is well seen from Fig. 8 which shows the density plot of the BEC density $|\psi(x, t)|^2$ associated with the second-order rational solution (12). It is observed from Figs. 7a and 7b that in the absence of the laser field ($m = 0$), the wave of
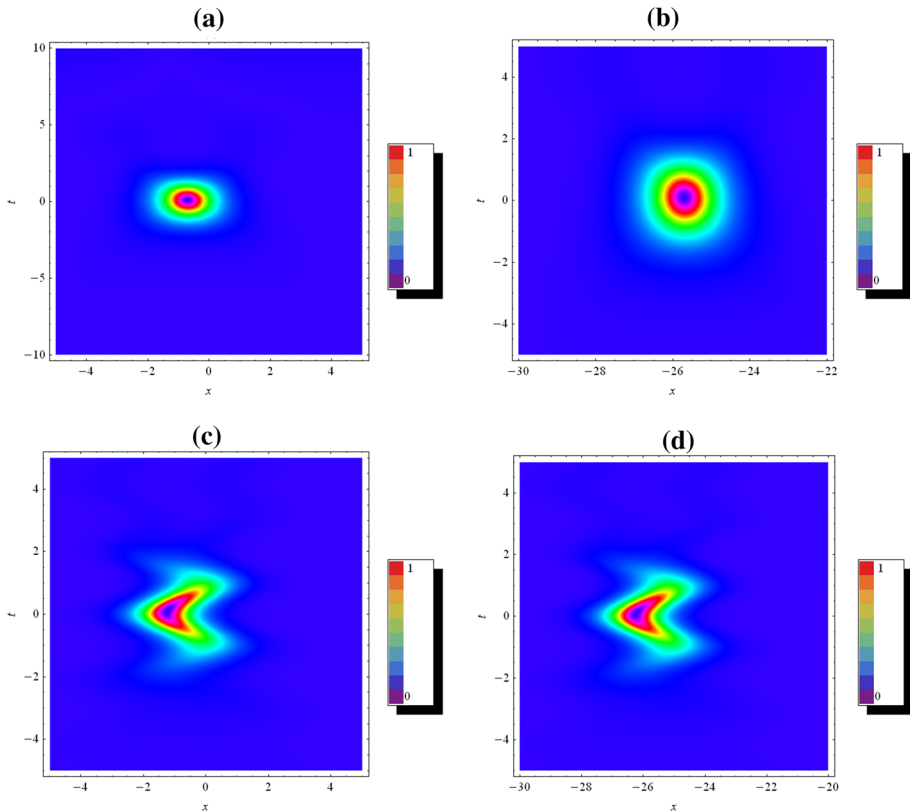
Fig. 8 Density plots for the BEC density $|\psi(x, t)|^2$ of the second-order dissipative forced rogue matter wave associated with the second-order rational solution (12) of the GP Eq. (1) with data (19) for the feeding parameter $\gamma(t) = -0.1$, which corresponds to $\kappa = 0.05$. The parameters are the same as those in Fig. 7

each of these plots appears from nowhere, then splits into two bright solitons each of which propagates along a parabolic trajectory (one in $+x$ direction and another one in $-x$ direction), and then fuse into a dark soliton which propagates along a straight line trajectory (in time). Figure 7b, as well as Fig. 8b show that the bias magnetic field delays the wave motion (that is, decreases the wave velocity) and enhances the region of the concentration of the BEC energy (this last behavior is well observed if comparing Fig. 8a obtained in the absence of the bias magnetic field with Fig. 8b generated in the presence of the bias magnetic field). Each of Figs. 7c and 7d show a wave, probably formed of the fusion of two bright solitons appearing from nowhere, which after a short time splits into two small bright solitons each of which propagates along an oscillating parabolic trajectory in the (x, t) space (one in $+x$ direction and the other one in $-x$ direction); after a certain time, these two bright solitons fuse in a dark soliton which propagates along an oscillating trajectory in the (x, t) space. The oscillations of the wave trajectories are induced by the laser field. Comparing either plots (a) and (c) or plots (b) and (d) of each of Figs. 7 and 8, it is well observed that the laser field also delays the wave motion (that is, decreases the wave velocity). Thus, the bias magnetic and laser fields have the same effect on the wave velocity. In passing, we note that the laser modulation frequency ω coincides with the trajectory frequency and seriously modifies the
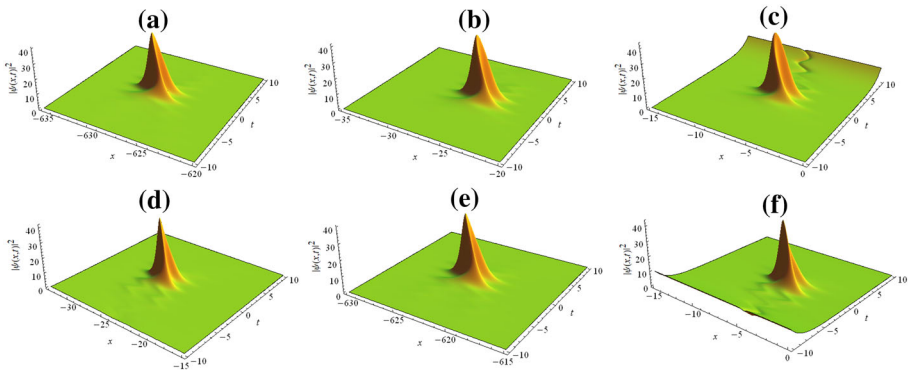
Fig. 9 Spatiotemporal evolution of the second-order dissipative forcing (top panels) and damped (bottom) rogue waves associated with the exact solution (12) for different values of the feeding/loss parameter κ with the same parameters as in Fig. 8d. **a**, **d**: $\kappa = \pm 0.01$, **b**, **e**: $\kappa = \pm 0.05$; (c), (f): $\kappa = \pm 0.1$. Positive κ is associated with BEC system with gain of atoms (top panels), while negative κ corresponds to BEC system with loss of atoms (bottom panels)

oscillation trajectory and the wave motion. We also point out that the wave velocity increases with the increasing the value of the frequency ω. For simplicity, we do not include the figures here.

For the above given set of parameters of the GP Eq. (1) with potential (3), the amplitude of the first- and second-order rogue matter waves associated with solutions (10) and (12) is proportional to $p(t) = \sqrt{2g(t)} \exp\left[-2 \int \gamma(t) \mathrm{d}t\right] = \sqrt{2g_{01}} \exp\left[3\kappa t\right]$. Because each of $\alpha(t)$, $\beta(t)$, and $T(t)$ given by Eq. (19) contains the expression $\exp\left[n\kappa t\right]$ ($n \in \{2, 4\}$), the fact that the wave amplitude is proportional to $p(t) = \sqrt{2g_{01}} \exp\left[3\kappa t\right]$ does not necessary mean that the wave amplitude will increase (decrease) either with time or with κ for BEC systems with feeding ($\kappa > 0$) (loss ($\kappa < 0$)) of atoms. For a better understanding, we show the spatiotemporal evolution of the second-order rogue wave in Fig. 9 for different values of the feeding/loss parameter κ, varying κ from $\kappa = \pm 0.01$ to $\kappa = \pm 0.1$. Plots of Fig. 9 reveal that for a given set of parameters of the BEC system and for a given set of the solution parameters, the second-order dissipative rogue waves have the same value of the main peak, independently of the value of the feeding/loss parameter κ. Therefore, the feeding and the loss of the BEC atoms does not affect the magnitude of the atomic density $|\psi(x,t)|^2$.

4 Conclusion

We have presented the exact analytical rogue wave solutions for the quasi-one-dimensional GP equation, which describes the evolution of cigar shaped BECs when either the gain or the lost of atoms is taken into consideration. These exact solutions have been obtained by combining the ansatz method and the similarity transformation technique and are valid in general for any form of the functional parameters, provided they obey certain conditions (integrability condition (8)). Using the exact solutions, we have exemplified the controllable behavior of dissipative rogue matter waves, with (i) time-independent harmonic confining potential, (ii) periodic nonlinearity, (iii) periodic linear confining potential, and (iv) combined time-independent harmonic repulsive and periodic linear potentials. Different potentials used in these examples are experimentally realizable. We then studied the characteristics of the

constructed dissipative rogue waves in detail. We have found that the external harmonic and linear trapping potentials can be used simultaneously to manipulate the motion of dissipative rogue matter waves in the BEC systems; we have also found that control of the scattering length allows us to manipulate the motion of dissipative rogue wave of the BEC systems. Our results reveal that the gain (loss) of the BEC atoms seriously modifies the nonzero cw backgrounds of the dissipative rogue waves, making them increasing (decreasing) during the wave motion. We also found that the dissipative term of the GP Eq. (1) does not affect the wave amplitude during its propagation, but affects the wave width. In the case of BECs in linear external potential (related to the bias magnetic field or/and the laser field), we found that the linear potential temporally and spatially affects the propagation of waves without affecting their amplitudes, except in the situation when the external potential consists of only the bias magnetic field. Developments of controlling the scattering length in the experiments allow for the experimental investigation of our prediction in the future. Because of the space-time modulated parameters in the GP Eq. (1), the results obtained in this work will be useful to study dissipative rogue waves in BECs experimentally and in other fields of nonlinear science.

Compliance with ethical standards

Conflicts of interest The author declares that he has no known competing financial interests or personal relationships that could have appeared to influence the work reported in this paper.

5 Appendix

5.1 On the first- and second-order rational solutions

Following the direct method developed by Akhmediev et al. [15], system (6a)–(6b) admits a first-order rational solution of form $(\psi_1, \psi_2) = (1, \varphi_0 T) \psi_1(X, T)$, with $\psi_1(X, T) = \rho_0 / (1 + aX^2 + bT^2)$, where φ_0, ρ_0, a, and b are real constants with $a > 0$ and $b > 0$. Asking that the pair (ψ_1, ψ_2) satisfies system (6a)–(6b) leads to $T_0 \lambda_0 - A_0^2 g_0 = 0$. Taking for simplicity $A_0 = \lambda_0 = 1$ and $g_0 = \frac{1}{2}$, and $T_0 = \frac{1}{2}$ yields $\rho_0 = -4/B_0$, $a = B_0^2 \rho_0^2 / 8 = 2$, $b = C_0 \varphi_0 (8\rho_0 + 3B_0 \rho_0^2) / 8 = 4$, $\varphi_0 = B_0^2 \rho_0 (8 + 3B_0 \rho_0) / (8C_0) = 2B_0/C_0$.

The real functions ψ_{11}, ψ_{ij}, and $\psi_{22}(X, T)$ appearing in Eq. (11a) are given by

$$\begin{pmatrix} \psi_{11}(X, T) \\ \psi_{ij}(X, T) \\ \psi_{22}(X, T) \end{pmatrix} = \begin{pmatrix} \frac{3(1-4X^2)+8T^2(8T^2-9)-4(X^2+6T^2)^2}{8B_0} \\ \frac{3}{32} + \frac{3(22T^2+3X^2)}{16} + \frac{(6T^2-X^2)^2}{8} + \frac{8T^6+12T^6X^2+6T^2X^4+X^6}{12} \\ \frac{15-8T^2+12X^2-(4T^2+2X^2)^2}{4C_0} \end{pmatrix}. \quad (A1)$$

5.2 Different parametric functions used in 3.1

For the gain (loss) parameter (14), we obtain from Eqs. (5b)–(7) that for $\gamma(t) = \gamma_-$,

$$
\begin{pmatrix} \alpha(t) \\ \beta(t) \\ T(t) \end{pmatrix} = \begin{pmatrix} 2\exp\left[\left(\sqrt{2\kappa} - 4\kappa\right)t\right] \\ \beta_{01} + \beta_{02}\exp\left[2\left(\sqrt{2\kappa} - 4\kappa\right)t\right] \\ \frac{1}{4\kappa - \sqrt{2\kappa}}\left(1 - \exp\left[2\left(\sqrt{2\kappa} - 4\kappa\right)t\right]\right) \end{pmatrix}, \tag{A2}
$$

and for $\gamma(t) = \gamma_+$,

$$
\begin{pmatrix} \alpha(t) \\ \beta(t) \\ T(t) \end{pmatrix} = \begin{pmatrix} 2\exp\left[-\sqrt{2\kappa}t\right] \\ \beta_{01} + \beta_{02}\exp\left[-2\sqrt{2\kappa}t\right] \\ T = \frac{1}{\sqrt{2\kappa}}\left(1 - \exp\left[-2\sqrt{2\kappa}t\right]\right) \end{pmatrix}, \tag{A3}
$$

where β_{01} and β_{02} are arbitrary real constants (it is preferable to use β_{01} and β_{02} which satisfy the condition $|\beta(t)| > 0$).

5.3 Different parametric functions used in 3.2

Employing Eqs. (5b)–(7) yields

$$
\begin{pmatrix} \alpha(t) \\ \beta(t) \\ T(t) \end{pmatrix} = \begin{pmatrix} 2\left(1 + m\sin[\omega t]\right)\exp\left[-2\gamma t\right] \\ \beta_{01} - 2\beta_{02}\left(\frac{2+m^2}{4\gamma} + \frac{4m(\omega\cos[\omega t]+4\gamma\sin[\omega t])}{\omega^2+16\gamma^2} + \frac{m^2(\omega\sin[2\omega t]-2\gamma\cos[2\omega t])}{2(\omega^2+4\gamma^2)}\right)\exp\left[-4\gamma t\right] \\ T_{10} - \left(\frac{2+m^2}{4\gamma} + \frac{4m(\omega\cos[\omega t]+4\gamma\sin[\omega t])}{\omega^2+16\gamma^2} + \frac{m^2(\omega\sin[2\omega t]-2\gamma\cos[2\omega t])}{2(\omega^2+4\gamma^2)}\right)\exp\left[-4\gamma t\right] \end{pmatrix},
$$
$$
\tag{A4}
$$

where, β_{01} and β_{02} are real constants (it is preferable to use β_{01} and β_{02} which satisfy the condition $|\beta(t)| > 0$) and $T_{10} = \frac{2+m^2}{4\gamma} + \frac{4m\omega}{\omega^2+16\gamma^2} - \frac{2m^2\gamma}{2(\omega^2+4\gamma^2)}$, so that $T(0) = 0$.

References

1. P. Müller, C. Garrett, A. Osborne, Rogue waves. Oceanography **18**, 66 (2005)
2. D.R. Solli, C. Ropers, P. Koonath, B. Jalali, Optical rogue waves. Nature **450**, 1054 (2007)
3. B. White, On the chance of freak waves at sea. J. Fluid Mech. **355**, 113 (1998)
4. N. Akhmediev, E. Pelinovsky, Introductory remarks on "Discussion and Debate: Rogue Waves - Towards a Unifying Concept?". Eur. Phys. J. Special Topics **185**, 1 (2010)
5. E. Kengne, W.M. Liu, Engineering rogue waves with quintic nonlinearity and nonlinear dispersion effects in a modified Nogochi nonlinear electric transmission network. Phys. Rev. E **102**, 012203 (2020)
6. E. Kengne, W.M. Liu, Transmission of rogue wave signals through a modified Noguchi electrical transmission network. Phys. Rev. E **99**, 062222 (2019)
7. L. Draper, 'Freak' ocean waves. Mar. Obs. **35**, 193 (1965)
8. Y.V. Bludov, V.V. Konotop, N. Akhmediev, Matter rogue waves. Phys. Rev. A. **80**, 033610 (2009)
9. J.S.-C.N. Akhmediev, A. Ankiewicz, Extreme waves that appear from nowhere: on the nature of rogue waves. Phys. Lett. A **373**, 2137 (2009)
10. N. Akhmediev, A. Ankiewicz, M. Taki, Waves that appear from nowhere and disappear without a trace. Phys. Lett. A **373**, 675 (2009)
11. A. Ankiewicz, N. Devine, N. Akhmediev, Are rogue waves robuste against perturbations? Phys. Lett. A **373**, 3997 (2009)
12. E. Kengne, W.M. Liu, Dissipative ion-acoustic solitons in ion-beam plasma obeying a κ-distribution. AIP Adv. **10**, 045218 (2020)

13. W.M. Liu, E. Kengne, *Schrödinger Equations in Nonlinear Systems* (Springer Nature, Singapore, 2019). https://doi.org/10.1007/978-981-13-6581-2

14. D.H. Peregrine, Water waves, nonlinear Schrödinger equations and their solutions. J. Aust. Math. Soc. Ser. B **25**, 16 (1983)

15. N. Akhmediev, A. Ankiewicz, J.M. Soto-Crespo, Rogue waves and rational solutions of the nonlinear Schrödinger equation. Phys. Rev. E **80**, 026601 (2009)

16. N. Akhmediev, A. Ankiewicz, M. Taki, Waves that appear from nowhere and disappear without a trace. Phys. Lett. A **373**, 675 (2009)

17. Z.Y. Yan, Nonautonomous "rogons" in the inhomogeneous nonlinear Schrödinger equation with variable coefficients. Phys. Lett. A **374**, 672 (2010)

18. Y.Y. Wang, C.Q. Dai, Spatiotemporal rogue waves for the variable-coefficient (3+1)-dimensional nonlinear Schrödinger. Equ. Commun. Theor. Phys. **58**, 255 (2012)

19. D.R. Solli, C. Ropers, P. Koonath, B. Jalali, Optical rogue waves. Nature (London) **450**, 1054 (2007)

20. Z.-Y. Yan, Financial rogue waves. Commun. Theor. Phys. **54**, 947 (2010)

21. N. Akhmediev, J.M. Soto-Crespo, A. Ankiewicz, Extreme waves that appear from nowhere: on the nature of rogue waves. Phys. Lett. A **373**, 2137 (2009)

22. S.Y. Song, J. Wang, J.M. Meng, J.B. Wang, P.X. Hu, Nonlinear Schrödinger equation for internal waves in deep sea. Acta Phys. Sin. **59**, 1123 (2010)

23. N. Song, Y. Xue, Discrete Dyn. Nat. Soc. **2016**, 7879517 (2016). https://doi.org/10.1155/2016/7879517

24. M.H. Anderson, J.R. Ensher, M.R. Matthews, C.E. Wieman, E.A. Cornell, Observation of Bose–Einstein condensation in a dilute atomic vapor. Science **269**, 198 (1995)

25. C.C. Bradley, C.A. Sackett, J.J. Tollett, R.G. Hulet, Evidence of Bose–Einstein condensation in an atomic gas with attractive interactions. Phys. Rev. Lett. **75**, 1687 (1995)

26. K.B. Davis, M.-O. Mewes, M.R. Andrews, N.J. van Druten, D.S. Durfee, D.M. Kurn, W. Ketterle, Bose–Einstein condensation in a gas of sodium atoms. Phys. Rev. Lett. **75**, 3969 (1995)

27. A. Mohamadou, E. Wamba, S.Y. Doka, T.B. Ekogo, T.C. Kofane, Generation of matter-wave solitons of the Gross–Pitaevskii equation with a time-dependent complicated potential. Phys. Rev. A **84**, 023602 (2011)

28. E. Kengne, A. Lakhssassi, R. Vaillancourt, W.M. Liu, Phase engineering, modulational instability, and solitons of Gross–Pitaevskii-type equations in 1+1 dimensions. J. Math. Phys. **54**, 051501 (2013)

29. E. Kengne, X.X. Liu, B.A. Malomed, S.T. Chui, W.M. Liu, Explicit solutions to an effective Gross–Pitaevskii equation: one-dimensional Bose-Einstein condensate in specific traps. J. Math. Phys. **49**, 023503 (2008)

30. E. Kengne, W.M. Liu, Management of matter-wave solitons in Bose–Einstein condensates with time-dependent atomic scattering length in a time-dependent parabolic complex potential. Phys. Rev. E **98**, 012204 (2018)

31. S. Serafini, L. Galantucci, E. Iseni, T. Bienaimé, R.N. Bisset, C.F. Barenghi, F. Dalfovo, G. Lamporesi, G. Ferrari, Vortex reconnections and rebounds in trapped atomic Bose–Einstein condensates. Phys. Rev. X **7**, 021031 (2017)

32. F. Dalfovo, S. Giorgini, L.P. Pitaevskii, S. Stringari, Theory of Bose–Einstein condensation in trapped gases. Rev. Mod. Phys. **71**, 463 (1999)

33. U. Roy, R. Atre, C. Sudheesh, C.N. Kumar, P.K. Panigrahi, Complex solitons in Bose–Einstein condensates with two- and three-body interactions. J. Phys. B **43**, 025003 (2010)

34. FKh Abdullaev, M. Salerno, Gap-Townes solitons and localized excitations in low-dimensional Bose–Einstein condensates in optical lattices. Phys. Rev. A **72**, 033617 (2005)

35. A.J. Moerdijk, B.J. Verhaar, A. Axelsson, Resonances in ultracold collisions of ^{6}Li, ^{7}Li, and ^{23}Na. Phys. Rev. A **51**, 4852 (1995)

36. FKh Abdullaev, J.G. Caputo, R.A. Kraenkel, B.A. Malomed, Controlling collapse in Bose–Einstein condensates by temporal modulation of the scattering length. Phys. Rev. A **67**, 013605 (2003)

37. D.S. Wang, X.-F. Zhang, P. Zhang, W.M. Liu, Matter-wave solitons of Bose–Einstein condensates in a time-dependent complicated potential. J. Phys. B **42**, 245303 (2009)

38. E. Kengne, P.K. Talla, Dynamics of bright matter wave solitons in Bose–Einstein condensates in an expulsive parabolic and complex potential. J. Phys. B **39**, 3679 (2006)

39. Z.X. Liang, Z.D. Zhang, W.M. Liu, Dynamics of a bright soliton in Bose–Einstein condensates with time-dependent atomic scattering length in an expulsive parabolic potential. Phys. Rev. Lett. **94**, 050402 (2005)

40. D. MollK, A.L. Gaeta, G. Fibich, Self-similar optical wave collapse: observation of the townes profile. Phys. Rev. Lett. **90**, 203902 (2003)

41. F.K. Abdullaev, A.M. Kamchatnov, V.V. Konotop, V.A. Brazhnyi, Adiabatic dynamics of periodic waves in Bose–Einstein condensates with time dependent atomic scattering length. Phys. Rev. Lett. **90**, 230402 (2003)

42. Z. Jie-Fang, D. Chao-Qing, Control of nonautonomous matter rogue waves. Acta Phys. Sin. **65**, 050501 (2016)

43. S. Loomba, H. Kaur, R. Gupta, C.N. Kumar, T.S. Raju, Controlling rogue waves in inhomogeneous Bose–Einstein condensates. Phys. Rev. E **89**, 052915 (2014)

44. L. Khaykovich, F. Schreck, G. Ferrari, T. Bourdel, J. Cubizolles, L.D. Carr, Y. Castin, C. Salomon, Formation of a matter-wave bright soliton. Science **296**, 1290 (2002)

45. L. Wu, J.-F. Zhang, L. Li, Modulational instability and bright solitary wave solution for Bose–Einstein condensates with time-dependent scattering length and harmonic potential. New J. Phys. **9**, 69 (2007)

46. A. Ankiewicz, D.J. Kedziora, N. Akhmediev, Rogue wave triplets. Phy. Lett. A **375**, 2782 (2011)

47. H. Saito, M. Ueda, Dynamically stabilized bright solitons in a two-dimensional Bose–Einstein condensate. Phys. Rev. Lett. **90**, 040403 (2003)

48. F.Kh. Abdullaev, J.C. Bronski, R.M. Galimzyanov, Dynamics of a trapped 2D Bose–Einstein condensate with periodically and randomly varying atomic scattering length. arXiv:cond-mat/0205464

49. G. Theocharis, Z. Rapti, P.G. Kevrekidis, D.J. Frantzeskakis, V.V. Konotop, Modulational instability of Gross–Pitaevskii-type equations in $1 + 1$ dimensions. Phys. Rev. A **67**, 063610 (2003)

50. H.M. Li, F.M. Wu, Soliton solutions of Bose–Einstein condensate in linear magnetic field and time-dependent laser field. Chin. Phys. Lett. **21**, 1425 (2004)

51. Q. Yang, J.-F. Zhang, Bose–Einstein solitons in time-dependent linear potential. Opt. Commun. **258**, 35 (2006)

52. E. Wamba, T.C. Kofané, A. Mohamadou, Matter-wave solutions of Bose–Einstein condensates with three-body interaction in linear magnetic and time-dependent laser fields. Chin. Phys. B **21**, 070504 (2012)